

# Experiment [IRS]: Determining Molecular Constants with Rotational-Vibrational Spectroscopy

Qianrui Li

October 30, 2023

## Abstract

The vibrational rotational spectrums of the HCl molecule and cigarette smoke were obtained in this experiment using a Fourier Transform Infrared Spectrometer (FTIR). For the HCl molecule, each peak in the spectrum split into two peaks because  $^{35}\text{Cl}$  had an isotope,  $^{37}\text{Cl}$ , which was heavier and had lower transition energy. The rotational constant in the ground vibrational state,  $B_0$ , and first excited state,  $B_1$ , of  $\text{HCl}^{35}$  were determined as  $10.3488 \pm 0.0110 \text{ cm}^{-1}$  and  $10.0456 \pm 0.0110 \text{ cm}^{-1}$  respectively, and were used to calculate the value of  $B_e$ , which was  $10.5003 \pm 0.0110 \text{ cm}^{-1}$ . The bond length in different vibrational level ( $r_0, r_1, r_e$ ), the equilibrium oscillation frequency  $\omega_e$ , anharmonicity constant  $x_e$ , zero-point energy  $G(0)$ , and force constant of  $\text{HCl}^{35}$  and  $\text{HCl}^{37}$  were calculated and compared with the literature value. The difference between the parameters of  $\text{HCl}^{35}$  and  $\text{HCl}^{37}$  were discussed. The spectrum of cigarette smoke was also obtained, and the peaks in the spectrum were assigned to the vibrational rotational transition of CO,  $\text{CO}_2$ , HCN,  $\text{CH}_4$ , and  $\text{H}_2\text{O}$ . The values of  $B_0, B_1, B_e, r_0, r_1, r_e, \omega_e, x_e, G(0)$ , and force constant of CO were calculated and compared with the value of HCl, and the difference between them was discussed.

## 1 Introduction

### Vibrational Energy

The vibrational population can be transferred from the ground state to a higher state by absorbing energies. The *fundamental absorption* described the transition from  $v=0$  to  $v=1$ , and the energy was usually in the range of  $500 \text{ cm}^{-1}$  to  $4000 \text{ cm}^{-1}$ , which was within the infrared region.

The energy levels for diatomic molecules in an anharmonic state could be expressed as shown in equation 1.

$$G(v) = (v + \frac{1}{2})\omega_e - (v + \frac{1}{2})^2\omega_e x_e \quad (1)$$

In the first part of the equation 1 represented the energy of a harmonic oscillator, while the second part was the correction term for an anharmonic oscillator. The energy of an anharmonic oscillator was lower than the energy of a harmonic oscillator with an amount depending on the anharmonic constant  $\omega_e x_e$ . The frequency of the anharmonic oscillator was shown as  $\omega_e$ . With equation 1, the ground state energy could be shown as equation 2 with  $v=0$ , and so as the first excitation state ( $v=1$ ) and the second excitation

state ( $v=2$ ).

$$G(0) = \frac{1}{2}\omega_e - \frac{1}{4}\omega_e x_e \quad (2a)$$

$$G(1) = \frac{3}{2}\omega_e - \frac{9}{4}\omega_e x_e \quad (2b)$$

$$G(2) = \frac{5}{2}(\omega_e - \frac{25}{4}\omega_e x_e) \quad (2c)$$

With equation 2, the energy of the fundamental absorption ( $v=0$  to  $v=1$ ) and the energy of the first overtone ( $v=0$  to  $v=2$ ) could be calculated as shown in equation 3.

$$G(0 \rightarrow 1) = G(1) - G(0) = \omega_e - 2\omega_e x_e \quad (3a)$$

$$G(0 \rightarrow 2) = G(2) - G(0) = 2(\omega_e - 3\omega_e x_e) \quad (3b)$$

### Rotational Energy

The rotational energy could be described using equation 4 for a diatomic molecule.

$$F(J) = B_v(J + 1) \quad (4)$$

In this equation,  $J$  was the rotational quantum number, while  $B_v$  was the rotational constant, which was related to the moment of inertia  $I$  as shown in equation 5.

$$B_v = \frac{h}{8\pi^2 c I} \quad (5a)$$

$$I = \mu r^2 \quad (5b)$$

### Transition Energy

Since the vibrational transition and the vibrational transition involved two very different frequencies. The energy for vibrational rotational transition could be expressed as equation 6, while the centrifugal distortion was ignored here.

$$S(v, J) = (v + \frac{1}{2})\omega_e - (v + \frac{1}{2})^2\omega_e x_e + B_v(J + 1) \quad (6)$$

The scale of the constant B would change with increasing vibrational state v because the bond length would increase when the molecule vibrates more violently due to the anharmonicity. Since the value of B depended on the bond length, B would be changed in different vibrational state, which could be quantified by the equation 7.

$$B_v = B_e - \alpha_e(v + \frac{1}{2}) \quad (7)$$

In this equation,  $B_e$  was the rotational constant for the ground state, while  $\alpha_e$  was the anharmonicity constant.

### Rotational Selection Rules

When there were two transitions, the rotational state J in the lower vibrational state would be denoted as double prime ( $J''$ ), while the rotational state J in the upper vibrational state would be denoted as prime ( $J'$ ).

The transition where  $\Delta J = 0$  was forbidden, meaning that transition from  $J''=1$  to  $J'=1$  was not allowed. For  $\Delta J = 1$  was allowed and would be shown in the spectrum. The P, Q, R branches were defined based on  $\Delta J$ :

1. P branch - A transition where  $\Delta J=-1$ , for example,  $J''=1$  to  $J'=0$ .
2. Q branch - A transition where  $\Delta J=0$ , for example,  $J''=1$  to  $J'=1$ .
3. R branch - A transition where  $\Delta J=+1$ , for example,  $J''=1$  to  $J'=2$ .

From equation 6, the energy of any rotational state  $J''$  in the ground vibrational state  $v=0$  and the energy of rotational state  $J'$  in  $v=1$  could be deduced as shown in equation 8.

$$S(0, J'') = \frac{1}{2}\omega_e - \frac{1}{4}\omega_e x_e + B_0(J + 1) \quad (8a)$$

$$S(1, J') = \frac{3}{2}\omega_e - \frac{9}{4}\omega_e x_e + B_1(J + 1) \quad (8b)$$

Therefore, the transition energy from  $J''$  to  $J'$  could be calculated by subtracting equation 8a from equation 8b as shown in equation 9

$$S(0, J'' \rightarrow 1, J') = \omega_e - 2\omega_e x_e + (B_1 - B_0)(J + 1) \quad (9)$$

In an R-branch,  $\Delta J = +1$ , so  $J' = J'' + 1$ . Therefore, the transition energy for an R-branch could be calculated as shown in equation 10 based on equation 9. In the following equation,  $J''$  was written as J for simplicity.

$$S(R(J)) = \omega_e - 2\omega_e x_e + B_1(J+1)(J+2) - B_0J(J+1) \quad (10)$$

In a P-branch,  $\Delta J = -1$ , so  $J' = J'' - 1$ . Therefore, the transition energy for an P-branch could be calculated as shown in equation 11 based on equation 9.

$$S(P(J)) = \omega_e - 2\omega_e x_e + B_1J(J-1) - B_0J(J+1) \quad (11)$$

The rotational constant  $B_0$  and  $B_1$  could be calculated respectively based on equation 10 and 11 as shown in equation 12.

$$S(R(J)) - S(P(J)) = 4B_1(J + 1/2) \quad (12a)$$

$$S(R(J)) - S(P(J+2)) = 4B_0(J + 3/2) \quad (12b)$$

These equations were linear, and the value of  $B_0$  and  $B_1$  could be obtained by plotting the  $R(J)$ - $P(J)$  against  $(J+1/2)$  and  $R(J)$ - $P(J+2)$  against  $(J+3/2)$  respectively. The slope of the plot was four times the rotational constant  $B_0$  and  $B_1$ .

## 2 Methodology

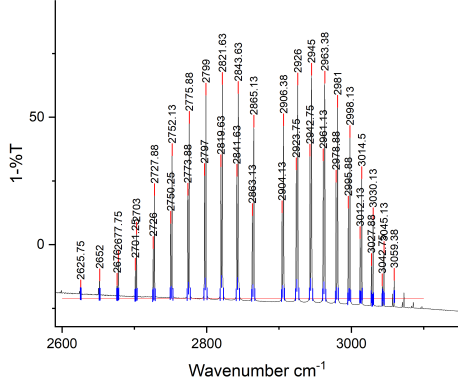
The 10  $\text{cm}^3$  gas cell was flushed with nitrogen and sealed with the Teflon lids. The background scan was performed with this cell using FT-IR spectrometer in the range  $6000 \text{ cm}^{-1}$  -  $2000 \text{ cm}^{-1}$  for 64 folds with resolution as 0.5. Three drops of concentrated HCl were added into the cell, and the spectrum was recorded under the same conditions.

The background scan was performed again under the same conditions with a larger gas cell. Cigarette smoke was captured in the cell using a tube to transform. The spectrum of cigarette smoke was recorded under the same conditions.

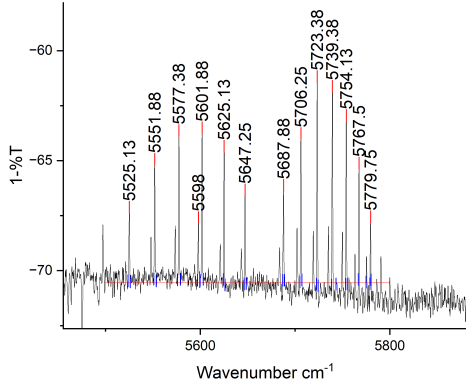
## 3 Results

The IR spectrum of HCl was recorded. The fundamental absorption of  $\text{HCl}^{35}$  was observed at  $2885.76 \text{ cm}^{-1}$ , while the first overtone was observed at  $5667.57 \text{ cm}^{-1}$ . The

fundamental absorption of  $\text{HCl}^{37}$  was observed at  $2883.51 \text{ cm}^{-1}$ , while the first overtone was observed at  $5665.32 \text{ cm}^{-1}$ . The spectrum of  $\text{HCl}$  were shown in Figure 1.



(a) Fundamental absorption.



(b) First overtone.

**Figure 1:** The IR spectrum of  $\text{HCl}$ . The plot (a) was the fundamental absorption, while (b) was the first overtone.

Since the P branch had a lower transition energy than the R branch, The peak with lower wavenumber would be P branch, while the peak with larger peak would be the R branch.

The wavenumber of the fundamental absorption for  $\text{HCl}^{35}$  and  $\text{HCl}^{37}$  were recorded separately in Table 1 and Table 2. The value of  $R(J)-P(J)$  and  $R(J)-P(J+2)$  were calculated to determine the rotational constant  $B_0$  and  $B_1$  for  $\text{HCl}^{35}$  and  $\text{HCl}^{37}$  respectively as shown in Table 1 and Table 2.

**Table 1:** The wavenumber of the fundamental absorption for  $\text{HCl}^{35}$  in P branch and R branch.

J	P ( $\text{cm}^{-1}$ )	R ( $\text{cm}^{-1}$ )	R(J)-P(J) ( $\text{cm}^{-1}$ )	R(J)-P(J+2) ( $\text{cm}^{-1}$ )
0	-	2906.38	-	62.75
1	2865.13	2926.00	60.87	104.37
2	2843.63	2945.00	101.37	146.00
3	2821.63	2963.38	141.75	187.50
4	2799.00	2981.00	182.00	228.87
5	2775.88	2998.13	222.25	270.25
6	2752.13	3014.50	262.37	311.50
7	2727.88	3030.13	302.25	352.38
8	2703.00	3045.13	342.13	-
9	2677.75	-	-	-

**Table 2:** The wavenumber of the fundamental absorption for  $\text{HCl}^{37}$  in P branch and R branch.

J	P ( $\text{cm}^{-1}$ )	R ( $\text{cm}^{-1}$ )	R(J)-P(J) ( $\text{cm}^{-1}$ )	R(J)-P(J+2) ( $\text{cm}^{-1}$ )
0	-	2904.13	-	62.50
1	2863.13	2923.75	60.62	104.12
2	2841.63	2942.75	101.12	145.75
3	2819.63	2961.13	141.50	187.25
4	2797.00	2978.88	181.88	228.63
5	2773.88	2995.88	222.00	269.88
6	2750.25	3012.13	261.88	310.88
7	2726.00	3027.88	301.88	351.88
8	2701.25	3042.75	341.50	-
9	2676.00	-	-	-

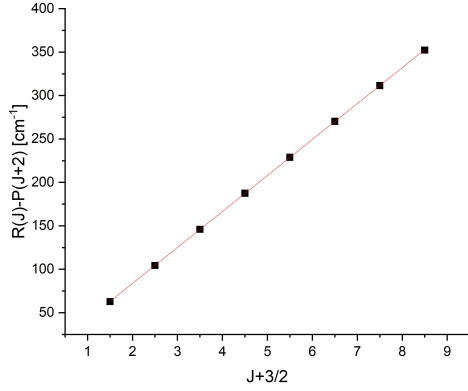
The rotational constant  $B_0$  could be obtained by plotting the  $R(J)-P(J)$  against  $(J+1/2)$  based on equation 12(a) as shown in Figure 2(a) for  $\text{HCl}^{35}$ . The rotational constant  $B_1$  could be obtained by plotting the  $R(J)-P(J+2)$  against  $(J+3/2)$  based on equation 12(b) as shown in Figure 2(b) for  $\text{HCl}^{35}$ .

The slope in Figure 2(a) was four times the rotational constant  $B_0$ , which was calculated as shown in equation 13.

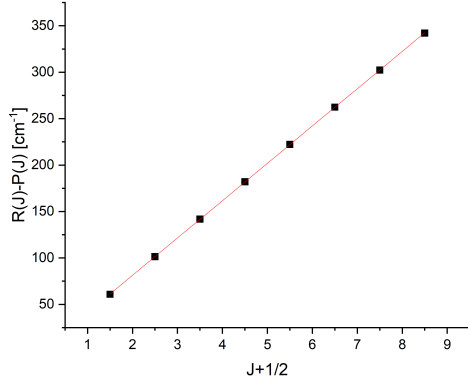
$$B_0 = \frac{41.3950 \pm 0.0442}{4} = 10.3488 \pm 0.0110 \text{ cm}^{-1} \quad (13)$$

The slope in Figure 2(b) was four times the rotational constant  $B_1$ , which was calculated as shown in equation 14.

$$B_1 = \frac{40.1825 \pm 0.0440}{4} = 10.0456 \pm 0.0110 \text{ cm}^{-1} \quad (14)$$



(a)  $R(J)-P(J+2)$  was plotted against  $(J+3/2)$ .



(b)  $R(J)-P(J)$  was plotted against  $(J+1/2)$ .

**Figure 2:** The rotational constant  $B_0$  and  $B_1$  for  $\text{HCl}^{35}$  were calculated based on the slope of the plot. The slope of plot (a) was  $41.3950 \pm 0.0442$  with  $r^2 = 1$ , which was four times the rotational constant  $B_0$ . The slope of plot (b) was  $40.1825 \pm 0.0440$  with  $r^2 = 0.99$ , which was four times the rotational constant  $B_1$ .

The rotational constant at equation,  $B_e$ , could be calculated based on  $B_0$  and  $B_1$  as shown in equation 15 based on equation 7.

$$10.3488 = B_e - \alpha_e(0 + 1/2) \quad (15a)$$

$$10.0456 = B_e - \alpha_e(1 + 1/2) \quad (15b)$$

The value of  $B_e$  was determined by solving these two equations, which was  $10.5003 \pm 0.0110 \text{ cm}^{-1}$ . The value of  $\alpha_e$  was also obtained as  $0.3029 \text{ cm}^{-1}$ .

The bond length of  $\text{HCl}$  in different vibrational could be calculated using  $B_0$ ,  $B_1$ , and  $B_e$  based on equation 5 respectively as shown in equation 16.

$$\mu = \frac{m_H m_{35}\text{Cl}}{m_H + m_{35}\text{Cl}} = 1.6266 \times 10^{-27} \text{ kg} \quad (16a)$$

$$r_0 = \sqrt{\left(\frac{h}{8\pi^2 \mu B_0 c}\right)} = 129.0 \text{ pm} \quad (16b)$$

$$r_1 = \sqrt{\left(\frac{h}{8\pi^2 \mu B_1 c}\right)} = 130.9 \text{ pm} \quad (16c)$$

$$r_e = \sqrt{\left(\frac{h}{8\pi^2 \mu B_e c}\right)} = 128.0 \text{ pm} \quad (16d)$$

The equilibrium oscillator frequency  $\omega_e$  and the anharmonic constant  $x_e$  could be calculated based on the energy of the fundamental absorption and the first overtone as shown in equation 3. The frequency of the fundamental absorption was  $2885.76 \text{ cm}^{-1}$ , while the frequency of the first overtone was  $5667.57 \text{ cm}^{-1}$ . The value of  $\omega_e$  and  $x_e$  were calculated as shown in equation 17.

$$2885.76 = \omega_e - 2\omega_e x_e \quad (17a)$$

$$5667.57 = 2(\omega_e - 3\omega_e x_e) \quad (17b)$$

$$\omega_e = 2989.70 \text{ cm}^{-1} \quad (17c)$$

$$\omega_e x_e = 51.9725 \text{ cm}^{-1} \quad (17d)$$

$$x_e = 0.0017384 \quad (17e)$$

The zero point energy of  $\text{HCl}^{35}$  could be calculated using equation 2(a) with the value of  $\omega_e$  and  $x_e$  as shown in equation 18.

$$G(0) = \frac{1}{2}\omega_e - \frac{1}{4}\omega_e x_e = 1494.86 \text{ cm}^{-1} \quad (18)$$

The force constant of  $\text{HCl}^{35}$  bond could be calculated as shown in equation 19 and the reduced mass ( $\mu$ ) of  $\text{HCl}^{35}$  was calculated as  $1.6273 \times 10^{-25}$ .

$$\nu = \frac{1}{2\pi} \sqrt{\frac{k}{\mu}} \quad (19a)$$

$$\nu = c/\lambda = c \times \text{wavenumber} \quad (19b)$$

$$\nu = 2.99792 \times 10^{10} \text{ cm} \cdot \text{s}^{-1} * 2885.76 \text{ cm}^{-1} = 8.65128 \times 10^{13} \text{ Hz} \quad (19c)$$

$$k = \mu \nu^2 (2\pi)^2 = 480.618 \text{ Nm}^{-1} \quad (19d)$$

The value of  $B_0$ ,  $B_1$ ,  $B_e$ ,  $\alpha_e$ ,  $r_0$ ,  $r_1$ ,  $r_e$ ,  $\omega_e$ ,  $x_e$ ,  $G(0)$ , and  $k$  for  $\text{HCl}^{35}$  were summarized in Table 3 and for  $\text{HCl}^{37}$  were calculated using the same method as shown in Table 3 and 4. This value was compared with the literature value.

**Table 3:** The value of  $B_0$ ,  $B_1$ ,  $B_e$ ,  $\alpha_e$ ,  $r_0$ ,  $r_1$ ,  $r_e$ ,  $\omega_e$ ,  $x_e$ ,  $G(0)$ , and  $k$  for  $\text{HCl}^{35}$ .

	$\text{HCl}^{35}$	Literature value	Error (%)
$B_0$ ( $\text{cm}^{-1}$ )	10.3488 $\pm 0.0110$	10.4404 <sup>1</sup>	0.9
$B_1$ ( $\text{cm}^{-1}$ )	10.0456 $\pm 0.0110$	10.1366 <sup>1</sup>	0.9
$B_e$ ( $\text{cm}^{-1}$ )	10.5003 $\pm 0.0110$	10.5923 <sup>1</sup>	0.9
$\alpha_e$ ( $\text{cm}^{-1}$ )	0.3029	0.3038 <sup>1</sup>	0.3
$r_0$ (pm)	129.0	-	-
$r_1$ (pm)	130.9	-	-
$r_e$ (pm)	128.0	127.46 <sup>2</sup>	0.4
$\omega_e$ ( $\text{cm}^{-1}$ )	2989.70	2990.95 <sup>2</sup>	0.04
$x_e$	0.017384	0.017659 <sup>2</sup>	1.6
$G(0)$ ( $\text{cm}^{-1}$ )	1494.86	-	-
$k$ ( $\text{Nm}^{-1}$ )	480.619	480.45 <sup>2</sup>	0.04

**Table 4:** The value of  $B_0$ ,  $B_1$ ,  $B_e$ ,  $\alpha_e$ ,  $r_0$ ,  $r_1$ ,  $r_e$ ,  $\omega_e$ ,  $x_e$ ,  $G(0)$ , and  $k$  for  $\text{HCl}^{37}$ .

	$\text{HCl}^{37}$	Literature value	Error (%)
$B_0$ ( $\text{cm}^{-1}$ )	10.3370 $\pm 0.0130$	10.4247 <sup>1</sup>	0.8
$B_1$ ( $\text{cm}^{-1}$ )	10.0334 $\pm 0.0144$	10.1214 <sup>1</sup>	0.9
$B_e$ ( $\text{cm}^{-1}$ )	10.4888 $\pm 0.0137$	10.5764 <sup>1</sup>	0.8
$\alpha_e$ ( $\text{cm}^{-1}$ )	0.3036	0.3033 <sup>1</sup>	0.1
$r_0$ (pm)	128.9	-	-
$r_1$ (pm)	130.9	-	-
$r_e$ (pm)	128.0	-	-
$\omega_e$ ( $\text{cm}^{-1}$ )	2987.39	-	-
$x_e$	0.017366	-	-
$G(0)$ ( $\text{cm}^{-1}$ )	1480.73	-	-
$k$ ( $\text{Nm}^{-1}$ )	480.6489	-	-

The IR spectrum of the cigarette was recorded, and part of the spectrum from  $2000 \text{ cm}^{-1}$  to  $4000 \text{ cm}^{-1}$  was shown in Figure 3.

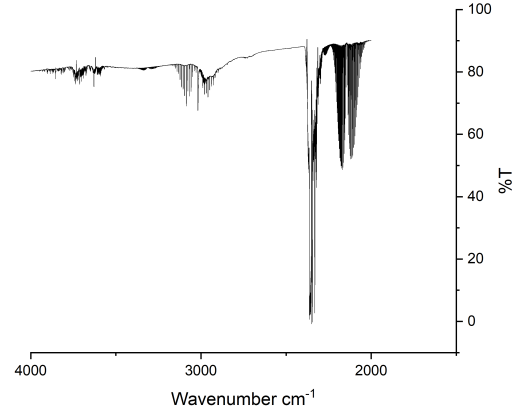


**Figure 3:** The IR spectrum of the cigarette.

The peaks were compared to the literature values and different gases in the cigarette were identified. The peak at  $2143.32 \text{ cm}^{-1}$  was identified as the fundamental absorption of CO as shown in Figure 4.

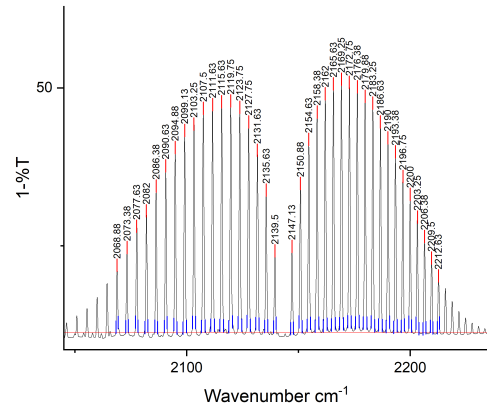


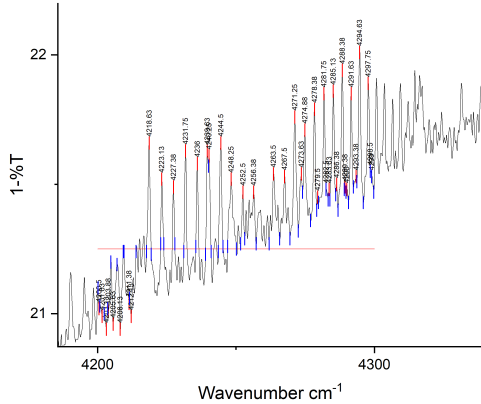
**Figure 4:** The IR spectrum of the fundamental absorption of CO.

The wavenumber of the fundamental absorption of the P-branch and R-branch for CO was recorded, and the value of  $R(J)$ - $P(J)$  was calculated as shown in Table 5.

**Table 5:** The wavenumber of the fundamental absorption for  $\text{HCl}^{37}$  in P branch and R branch.

J	P ( $\text{cm}^{-1}$ )	R ( $\text{cm}^{-1}$ )	R(J)-P(J) ( $\text{cm}^{-1}$ )	R(J)-P(J+2) ( $\text{cm}^{-1}$ )
0	-	2147.13	-	11.50
1	2139.50	2150.88	11.38	19.25
2	2135.63	2154.63	19.00	26.88
3	2131.63	2158.38	26.75	34.63
4	2127.75	2162.00	34.25	42.25
5	2123.75	2165.63	41.88	50.00
6	2119.75	2169.25	49.50	57.62
7	2115.63	2172.75	57.12	65.25
8	2111.63	2176.38	64.75	73.13
9	2107.50	2179.88	72.38	80.75
10	2103.25	2183.25	80.00	-
11	2099.13	-	-	-

The peak at  $4259.94 \text{ cm}^{-1}$  was identified as the first overtone of CO as shown in Figure 5.



In the IR spectrum of HCl, each large peak of the fundamental absorption for HCl was followed by a smaller peak as shown in Figure 1. This was because Cl had an isotope  $^{37}\text{Cl}$  with an abundance 24.23%, while  $^{35}\text{Cl}$  had an abundance as 75.77%. Since  $^{37}\text{Cl}$  was heavier than  $^{35}\text{Cl}$ , the reduced mass of  $\text{HCl}^{37}$  was greater than the reduced mass of  $\text{HCl}^{35}$ . Therefore, the rotational constant (B) of  $\text{HCl}^{37}$  would be lower than the rotational constant of  $\text{HCl}^{35}$  because B was dependent on the reduced mass of the molecule based on equation 5. The energy absorption of  $\text{HCl}^{37}$  would be lower than the energy absorption of  $\text{HCl}^{35}$  based on equation 6. Therefore, the split peak with a smaller wavenumber would be the vibrational-rotational spectrum of  $\text{HCl}^{37}$ , while the split peak with a larger wavenumber would be the vibrational-rotational spectrum of  $\text{HCl}^{35}$ .

The bond length of  $\text{HCl}^{37}$  and  $\text{HCl}^{35}$  were almost the same because  $^{37}\text{Cl}$  was an isotope of  $^{35}\text{Cl}$ , meaning that the chemical properties of  $^{37}\text{Cl}$  and  $^{35}\text{Cl}$  were similar.

The equilibrium oscillation frequency,  $\omega_e$ , of  $\text{HCl}^{37}$  was smaller than the equilibrium oscillation frequency of  $\text{HCl}^{35}$  because  $^{37}\text{Cl}$  was heavier than  $^{35}\text{Cl}$ , resulting in slower vibration. This resulted in the smaller value of zero-point energy of  $\text{HCl}^{37}$  than the zero-point energy of  $\text{HCl}^{35}$  because the zero-point energy was dependent on the equilibrium oscillation frequency based on equation 2(a).

The force constant of  $\text{HCl}^{37}$  was slightly greater than the force constant of  $\text{HCl}^{35}$  because the reduced mass of  $\text{HCl}^{37}$  was greater than the reduced mass of  $\text{HCl}^{35}$ , resulting in greater force constant based on equation 19.

In the spectrum of cigarettes, each peak was identified as different gases in the cigarette and compared to the literature value as shown in Table 7.

**Table 7:** The wavenumber of gases in the cigarette measured in the experiment and the literature value.

Gas	Experimental Data ( $\text{cm}^{-1}$ )	Literature value ( $\text{cm}^{-1}$ )	Error (%)
CO	2143.3	2143.7 <sup>5</sup>	0.03
CO <sub>2</sub>	2349.6	2349.3 <sup>5</sup>	0.01
CH <sub>4</sub>	3017.6	3020.3 <sup>5</sup>	0.09
HCN	3313.19	3311.5 <sup>5</sup>	0.05
H <sub>2</sub> O	3613.7	-	-

The experimental data was close to the literature value with a small error, which indicated that the experimental data was accurate.

The rotational constant  $B_v$  of CO was much smaller than the rotational constant of HCl. For a CO molecule, the difference between carbon and oxygen was small, meaning that the rotational center of the molecule would be close to the middle point of the two molecules. However, for an

HCl molecule, the mass of chlorine was much larger than the mass of hydrogen, indicating that the rotational center of the molecule would be very close to chlorine. When the HCl molecule rotated, the chlorine atom would be almost static, while the hydrogen would rotate around the chlorine atom. The reduced mass of CO was much greater than the reduced mass of HCl. This resulted in the smaller rotational constant of CO than the rotational constant of HCl as the rotational constant depended on the reduced mass of the molecule based on equation 5.

The bond length of the HCl was larger than the bond length of CO. This was because the bond length of a diatomic molecule was mainly dependent on the atomic radius of the two atoms. The atomic radius of chlorine was much larger than the atomic radius of oxygen and carbon because chlorine was in the third period and had one more electron shell filled with electrons, while oxygen and carbon were in the second period. Thus, the bond length of HCl would be greater than the bond length of CO.

The equilibrium oscillation frequency,  $\omega_e$ , of CO was smaller than the equilibrium oscillation frequency of HCl because hydrogen was much lighter than carbon and oxygen, resulting in faster vibration.

Since the value of  $\omega_e$  of CO was smaller than the value of  $\omega_e$  of HCl, the zero-point energy of CO was smaller than the zero-point energy of HCl based on equation 2(a).

The force constant of CO was much larger than the force constant of HCl because the reduced mass of CO was greater than the reduced mass of HCl, resulting in a larger force constant based on equation 19.

The calculated parameters for  $\text{HCl}^{35}$ ,  $\text{HCl}^{37}$ , and CO were compared with the literature value as shown in Tables 3, 4, and 6. The error for each parameter was very small, which indicated that the experimental data was accurate. This might be due to the high resolution of the spectrum, which could give a clear structure of the spectrum and make the analysis of the spectrum more accurate.

In this experiment, one possible experimental error might be that the sample was not fully evaporated, which would lead to a lower resolution and might affect the analysis of the spectrum. This could be improved by increasing the time for waiting before starting to record the spectrum to ensure that the sample was fully evaporated. Another possible error would be that air might be introduced into the sample, and some molecules in the air might also shown in the spectrum which would affect the analysis of the spectrum. To limit the air introduced into the sample, the speed of adding the sample into the cell could be faster. During the recording of the spectrum for cigarettes, the sample might leak out of the sample cell, which would lead to a lower resolution, and gases with low concentrations might not be shown in the spectrum. This could be improved by ensuring that the sample was fully sealed before recording the spectrum.

This experimental setup could be used in industrial

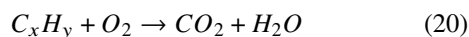
applications to identify the impurities in a sample as the vibrational-rotational spectrum of each molecule was unique. The spectrum could also be used to monitor the reaction process as the vibrational-rotational spectrum of the reactants and products were different. Therefore, the concentration of the reactants and products could be calculated respectively through the spectrum, which could reveal the reaction process.

In this experiment, the vibrational-rotational spectrum of HCl and cigarette were obtained and analysed. The vibrational-rotational spectrum of HCl was split into two peaks due to the different isotopes of chlorine. The fundamental absorption of  $\text{HCl}^{35}$  was  $2885.76\text{ cm}^{-1}$ , while the fundamental absorption of  $\text{HCl}^{37}$  was  $2883.63\text{ cm}^{-1}$ . The first overtone of  $\text{HCl}^{35}$  was  $5663.50\text{ cm}^{-1}$ , while the first overtone of  $\text{HCl}^{37}$  was  $5667.57\text{ cm}^{-1}$ . The value of  $B_0$ ,  $B_1$ ,  $B_e$ ,  $\alpha_e$ ,  $r_0$ ,  $r_1$ ,  $r_e$ ,  $\omega_e$ ,  $x_e$ ,  $G(0)$ , and  $k$  for  $\text{HCl}^{35}$  and  $\text{HCl}^{37}$  were calculated and compared with the literature value. The vibrational-rotational spectrum of the cigarette was analysed and the gases in the cigarette were identified as  $\text{CO}$ ,  $\text{CO}_2$ ,  $\text{CH}_4$ ,  $\text{HCN}$ , and  $\text{H}_2\text{O}$ . The wavenumber of each gas was compared to the literature value. The vibrational-rotational spectrum of  $\text{CO}$  was also analysed and the value of  $B_0$ ,  $B_1$ ,  $B_e$ ,  $\alpha_e$ ,  $r_0$ ,  $r_1$ ,  $r_e$ ,  $\omega_e$ ,  $x_e$ ,  $G(0)$ , and  $k$  for  $\text{CO}$  were calculated and compared with the literature value. The differences and trends of the parameters were discussed. The error for each parameter was very small, which indicated that the experimental data was accurate.

## 5 Investigation Question

In the industrial, FTIR could give information about complete and incomplete combustion, which would be discussed below.

During the complete combustion, the fuel would be fully oxidized to carbon dioxide and water as shown in equation 20.



The fuel usually not only contained carbon and hydrogen, but also contained other elements such as nitrogen, sulfur, and oxygen. Thus, nitrogen dioxide might also be produced during the complete combustion.<sup>6</sup>

If the combustion was incomplete, carbon monoxide would be produced instead of carbon dioxide, and other nitrogen oxides ( $\text{NO}_x$ ) might also exist.<sup>6</sup> Methane was also an important product during the incomplete combustion as shown in the equation.<sup>7</sup>

The sample after combustion could be analysed using FTIR. The representative peaks in the spectrum could be identified as compared to the literature value. The peak from  $2200\text{ cm}^{-1}$  to  $2400\text{ cm}^{-1}$  represented carbon dioxide, while the peak from  $2000\text{ cm}^{-1}$  to  $2200\text{ cm}^{-1}$  represented

carbon monoxide. Peaks from  $2300\text{ cm}^{-1}$  to  $3000\text{ cm}^{-1}$  could be assigned to aliphatic carbons.<sup>8</sup> The fundamental absorption of OH stretch for  $\text{H}_2\text{O}$  was around  $3500\text{ cm}^{-1}$ .<sup>9</sup> The peak around  $3020.3\text{ cm}^{-1}$  was correspond to  $\text{CH}_4$ .<sup>5</sup>

The main difference between complete and incomplete combustion was the production of carbon dioxide or carbon monoxide. Therefore, the analysis could focus on the amount of carbon dioxide and carbon monoxide. The concentration of the gases could be determined using the peak area of the fundamental absorption based on the Beer-Lambert law as shown in equation 21.<sup>10</sup>

$$A = \epsilon cl \quad (21)$$

The ratio of carbon dioxide and carbon monoxide could be calculated by knowing the concentration of both gases, which could be used to determine whether the combustion was complete or incomplete.

This experiment could reveal the concentration of carbon dioxide, which was the main product of complete combustion, and carbon monoxide, which was the main product of incomplete combustion. Thus, it could monitor the process of combustion. The combustion would tend to be complete if the temperature increased. Therefore, this experiment could also be used to determine at which temperature the combustion was fully complete.<sup>8</sup> However, if there were too many gases in the sample, the spectrum might be too complicated to analyse. Besides, this experiment could only measure gas but not liquid or solid, and also the gas without dipole moment would not shown in the spectrum as well. However, during incomplete combustion, carbon might also form, which could not be shown in the spectrum. Therefore, this experiment could only be used to measure the gas with dipole moment. The carbon dioxide might also be produced during incomplete combustion, which might be difficult to analyse.

To improve the reliability of the results, TGA-FTIR could be used.<sup>11</sup> Another method called PCFC-FTIR was also an alternative method to improve the reliability of the results.<sup>7</sup>

## References

- [1] E. D. T. Earle K. Plyler, *Z. Elektrochem. angew. phys. Chem.*, 1960, **64**, 717–720.
- [2] G. Herzberg, *Molecular Spectra and Molecular Structure — I Spectra of Diatomic Molecules*, D.vanNostrand, New York, 2nd edn., 1950.
- [3] N. Mina-Camilde, C. Manzanares I. and J. F. Caballero, *Journal of Chemical Education*, 1996, **73**, 804.
- [4] D. Rank, A. Pierre and T. Wiggins, *Journal of Molecular Spectroscopy*, 1965, **18**, 418–427.
- [5] A. R. Ford, W. A. Burns and S. W. Reeve, *Journal of Chemical Education*, 2004, **81**, 865.



- [6] I. Oluwoye, M. Altarawneh, J. Gore and B. Z. Dlugogorski, *Fuel*, 2020, **274**, 117805.
- [7] R. Sonnier, G. Dorez, H. Vahabi, C. Longuet and L. Ferry, *Combustion and Flame*, 2014, **161**, 1398–1407.
- [8] A. Decimus, R. Sonnier, P. Zavaleta, S. Suard and L. Ferry, *JOURNAL OF THERMAL ANALYSIS AND CALORIMETRY*, 2019, **138**, 753–763.
- [9] I. M. McIntosh, A. R. Nichols, K. Tani and E. W. Llewellyn, *American Mineralogist*, 2017, **102**, 1677–1689.
- [10] M. R. Roussel, *A Life Scientist's Guide to Physical Chemistry*, Cambridge University Press, Cambridge, 1st edn., 2012.
- [11] C. A. Wilkie, *Polymer Degradation and Stability*, 1999, **66**, 301–306.